NJC

Accepted Manuscript

This is an *Accepted Manuscript*, which has been through the Royal Society of Chemistry peer review process and has been accepted for publication.

Accepted Manuscripts are published online shortly after acceptance, before technical editing, formatting and proof reading. Using this free service, authors can make their results available to the community, in citable form, before we publish the edited article. We will replace this *Accepted Manuscript* with the edited and formatted *Advance Article* as soon as it is available.

You can find more information about *Accepted Manuscripts* in the Information for Authors.

Please note that technical editing may introduce minor changes to the text and/or graphics, which may alter content. The journal's standard Terms & Conditions and the Ethical guidelines still apply. In no event shall the Royal Society of Chemistry be held responsible for any errors or omissions in this *Accepted Manuscript* or any consequences arising from the use of any information it contains.

ROYAL SOCIETY OF CHEMISTRY

www.rsc.org/njc

A new synthesis method for crystalline mesoporous hematite film with controllable thickness is reported.

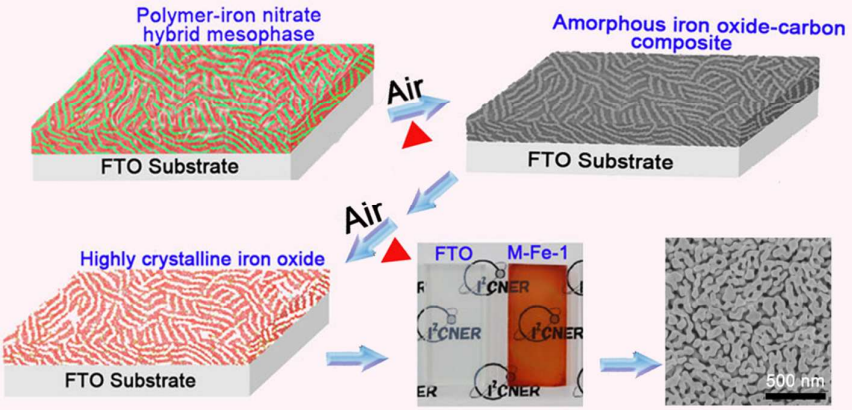

NJC

RSCPublishing

LETTER

Soft-templating Method to Synthesize Crystalline Mesoporous α-Fe_2O_3 Film

Cite this: DOI: 10.1039/c3nj00000x

Limin Guo,[a,*] Shintaro Ida,[b] Akihide Takashiba,[b] Takeshi Daio,[c] Norio Teramae,[d,*] and Tatsumi Ishihara[a,*]

Received 00th XXXXX 2013,
Accepted 00th XXXXX 2013

DOI: 10.1039/c3nj00000x

www.rsc.org/njc

Crystalline mesoporous α-Fe_2O_3 film is successfully synthesized using lab-synthesized di-block amphiphilic polymer poly(ethylene oxide)-b-poly(butyl acrylate) (PEO-b-PtBA) as a mesoporous structure directing agent and the film thickness can be adjusted by the repeated spin-coatings.

Synthesis of crystalline mesoporous metal oxide films has attracted much attention due to their intrinsic structural characteristics (well-defined mesoporosity and pore size) and their potential applications in catalysis, sensors, electronics and optics.[1-4] To date, many metal oxide films have been made by means of evaporation-induced self-assembly method (EISA).[5-10] However, except the studies by Bresesinski's group or related groups,[4-10] few studies on the metal oxide films with well-defined mesoporous structure and highly crystalline wall were still rarely reported. The reason is very likely due to the limited use of the special di-block copolymer of poly(ethylene-co-butylene)-block-poly(ethylene oxide)[11] (so called KLE and made by polymerization of ethylene oxide on a hydroxyl-terminated poly(ethylene-co-butylne) (Kraton Liquid)) as a structure-direct agent (SDA). To facilitate the research and applications, the synthesis of the mesoporous metal oxide film using other SDAs is highly desired. Herein, we report the crystalline mesoporous α-Fe_2O_3 film synthesis using the lab-synthesized amphiphilic di-block copolymer PEO-b-PtBA as the SDA. The PEO-b-PtBA was synthesized by the atom transfer radical polymerization method which is a popular to synthesize multi-block polymer with high quality.[12,13]

Figure 1a shows the schematic illustration of the synthesis of crystalline mesoporous α-Fe_2O_3 film. At first, a homogeneous polymer (PEO-b-PtBA) -iron nitrate hybrid film was spin-coated on the fluorine-doped tin oxide (FTO) glass substrate. Then, as the second step, the film was aged at 250°C for 12 h to strengthen or reconsolidate the structure of iron oxide-carbon rich composite. Thereafter, the film can be spin-coated again or more after repeating the second step to increase the thickness of the film. Finally, the film was calcined at 700°C to obtain the crystalline iron oxide and completely remove the template. The mesoporous α-Fe_2O_3 film samples obtained by repeat spin-coatings once, twice and three times are named as M-Fe-1, M-Fe-2 and M-Fe-3, respectively. The experimental details on the synthesis of PEO-b-PtBA are described in the Electronic Supplementary Information (ESI). Figure 1b shows a photo of the as-prepared mesoporous α-Fe_2O_3 film samples. After the formation of the mesoporous α-Fe_2O_3 film on FTO (M-Fe-1), the colour is changed into red. The red colour of M-Fe-2 and M-Fe-3 becomes deeper due to the increasing thickness of the mesoporous α-Fe_2O_3 film. The overall transparent characteristic feature reflects the homogeneity and integrity of these as-prepared films.

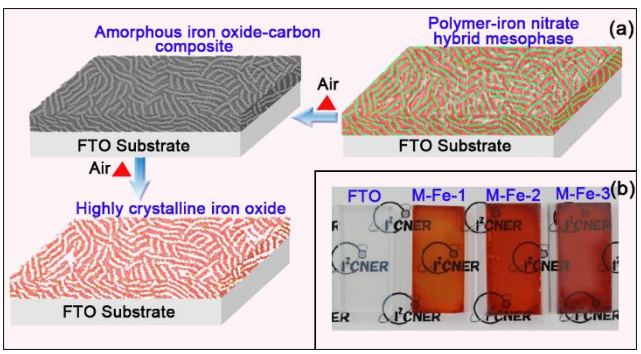

Fig. 1. (a) Schematic illustration of the synthesis of crystalline mesoporous α-Fe_2O_3 film; (b) The overview of as-synthesized mesoporous α-Fe_2O_3 Film on an FTO glass substrate.

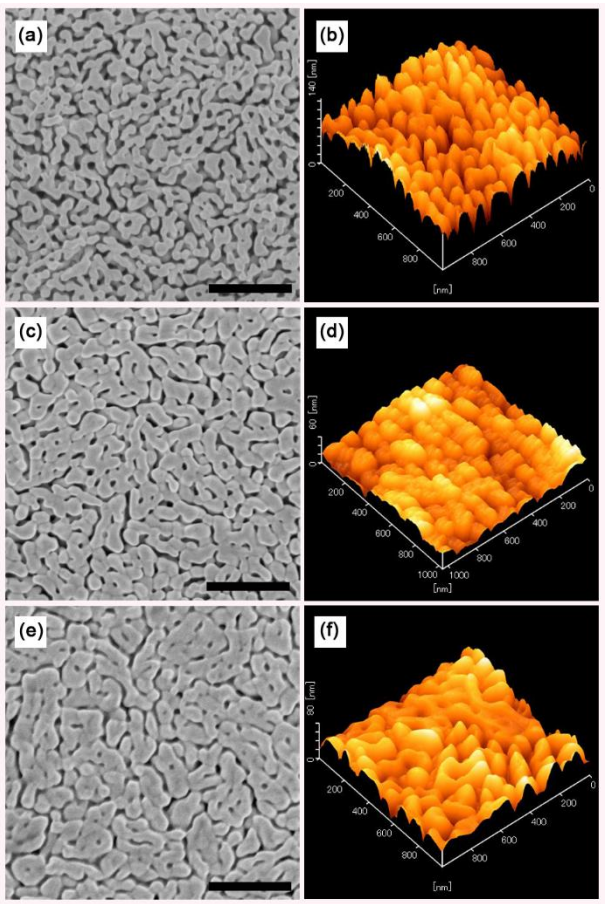

Fig. 2. The SEM and AFM images of M-Fe-1 (a, b), M-Fe-2 (c, d) and M-Fe-3 (e, f). The scale bar corresponds to 500 nm.

Figure 2 shows the scanning electron microscope (SEM) and atomic force microscope (AFM) images of mesoporous α-Fe_2O_3 film samples. Clear disordered and worm-like mesoporous channels can be clearly recognized in the SEM images (Figs.2a, 2c and 2e). The pore sizes evaluated by SEM observation are 30-60 nm, 20-40 nm and 15-35 nm for samples M-Fe-1, M-Fe-2 and M-Fe-3, respectively. After the aging at 250 °C, the PEO-b-PtBA used as an SDA was partially decomposed, which can be recognized as unfilled space in Fig. 2a. The unfilled space is stepwisely impregnated by twice and third times spin-coatings of the precursor solution as shown in Figs. 2c and 2e, and the space turns to porous channels after calcination of SDA. This phenomenon has been utilized to embed some nanoparticles into the mesochannels.[14] This should be the main reason why the pore size decreased with increasing spin-coating times. In the AFM images of samples M-Fe-1 (Fig.2b), M-Fe-2 (Fig.2d) and M-Fe-3 (Fig. 2f), clear three dimensional surface images of these porous films and round smooth frameworks (pore walls) can be observed. The cross section SEM images of the samples (ESI Fig.2) showed the mesoporous structure through the films. At the same time, the thickness of the pore wall monotonously increased from M-Fe-1 to M-Fe-3. The film thickness of M-Fe-1, M-Fe-2 and M-Fe-3 are around 180, 493 and 744 nm, respectively. The well-defined worm-like mesoporous structure is successfully synthesized and the film thickness can be increased by repeated spin-coatings. Notably, many former researches demonstrated crystalline pore wall formation usually leaded to the porous structural collapse.[15,16]

The XRD patterns of as-synthesized mesoporous α-Fe_2O_3 films (Fig. 3) show clear diffraction peaks, which can be well ascribed to SnO_2 and α-Fe_2O_3. In addition, the intensity of diffraction peaks corresponding to α-Fe_2O_3 increased from sample M-Fe-1 to M-Fe-3 and those for SnO_2 decreased at the same time, which is consistent with the fact that the α-Fe_2O_3

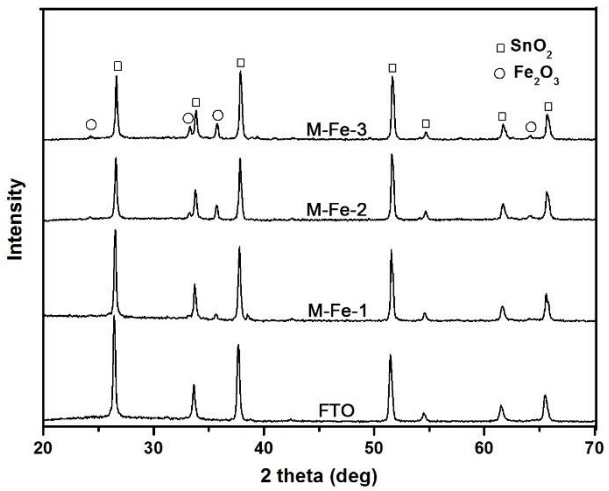

Fig. 3. XRD patterns of as-synthesized mesoporous α-Fe_2O_3 film and bare FTO substrate.

film thickness increased from M-Fe-1 to M-Fe-3 (ESI Fig. 2). The TEM analysis results of M-Fe-2 (ESI Fig. 3) show overall particles morphology and well crystalline structure. The porous structure was very likely destroyed during the film removal from the FTO substrate. The TEM analysis results of M-Fe-3 (ESI Fig. 4) also show well crystalline structure. In addition, the porous structure was maintained (ESI Fig. 4a), which was different from that of M-Fe-2 and might be ascribed to the thicker α-Fe_2O_3 film of M-Fe-3. Up to now, we can say the well-defined mesoporous α-Fe_2O_3 film with crystalline wall has been successfully synthesized. The thickness of the film can be increased by the repeated spin-coatings. The as-prepared α-Fe_2O_3 film without 700°C calcination has also been characterized. The XRD pattern of the sample M-Fe-3-N (ESI Fig. 5) (after the 250°C heat treatment) demonstrated amorphous state and SEM image (ESI Fig. 6) showed quite different surface from those of M-Fe-1, M-Fe-2 and M-Fe-3 (Fig. 2). Although the final mesoporous structure of the crystalline α-Fe_2O_3 film should originate from the inorganic (α-Fe_2O_3 related species) and organic (PEO-b-PtBA) hybrid mesophase, there should be an obvious change in the porous structure during the crystallization at high temperature. In order to evaluate the surface area of as-synthesized crystalline mesoporous α-Fe_2O_3 film, the crystalline mesoporous α-Fe_2O_3 powder was also synthesized by the same procedure and the same precursor solution as those used for M-Fe-1. From the SEM image and N_2 sorption isotherm of as-synthesized crystalline mesoporous α-Fe_2O_3 powder (ESI Fig. 7), clear

mesoporous structure was recognized, and the surface area was 18 m^2/g and the pore size was around 45 nm. There are two main different points for the crystalline mesoporous α-Fe_2O_3 films between previous study[17] using KLE as an SDA and the present study. The mesochannels of α-Fe_2O_3 films reported here are worm-like or disordered and the pore size is changeable by repeated spin-coatings. The mesochannels of the reported α-Fe_2O_3 film are ordered and the pore size is kept constant.[17]

The as-synthesized PEO-b-PtBA amphiphilic polymer can also be used as the SDA to synthesize the mesoporous silica film. From the SEM images of as-synthesized mesoporous silica films (ESI, Figs. 8 and 9) prepared by using tetrafuran (film name is M-Si-THF) and ethanol (M-Si-EtOH) as an evaporating solvent, and the pore size and the thickness of M-Si-THF were respectively estimated as 15 nm and 120 nm. The pore size and the thickness of M-Si-EtOH were 15 nm and 540 nm, respectively.

The α-Fe_2O_3 based electrodes used in solar water splitting have emerged as one of the most promising materials.[18-20] Figure 4 is the current-potential curves of M-Fe-1 to show the water oxidation by photoelectrochemical process. The sample yielded a photocurrent density of 85 μA/cm^2 at 0.8 V vs SCE, which shows an obvious increase compared to the bare FTO. Nevertheless, the value is still relatively low and the value showed no further improvement when the α-Fe_2O_3 thickness was increased (ESI Fig.10). The reason may be due to the poor conductivity of the mesoporous α-Fe_2O_3. Further improvement in the conductivity of mesoporous α-Fe_2O_3 could be achieved by modification of some efficient co-catalysts. We are now undertaking further studies in this direction.

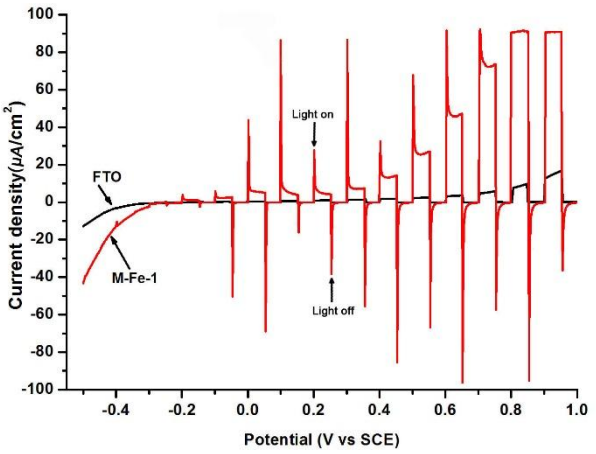

Fig.4. Photochemical performance of M-Fe-1 and bare FTO substrate.

In summary, nanoporous crystalline α-Fe_2O_3 films on FTO substrate were successfully synthesized using lab-synthesized amphiphilic polymer PEO-b-PtBA and the film thickness could be adjusted by repeated spin-coatings. The pore size decreased with increasing the number of spin-coating times. The PEO-b-PtBA can be also used for the synthesis of mesoporous silica films as an SDA.

Experimental section

The preparation of crystalline mesoporous α-Fe_2O_3 film: 80 mg of PEO-b-PtBA was dissolved in the mixture of 3.0 mL of ethanol and 1.0 mL of 2-methoxyethanol. Then, 836 mg $Fe(NO_3)_3{\cdot}9H_2O$ was added into above solution. After the dissolution of $Fe(NO_3)_3{\cdot}9H_2O$, the films were prepared by spinning coating on fluorine-doped tin oxide (FTO) glass substrates. Later, the films were aged at 250 °C for 12 h and thereafter calcined at 700 °C for 30 min. The obtained film was named as M-Fe-1 for simplicity. After the aging at 250 °C, the films can be used for the second spinning coating in order to get the thicker film and then calcined at 700 °C for 30 min. The obtained film was named as M-Fe-2. After aging at 250 °C, the film spin-coated twice was used for the third spin-coating and then calcined at 700 °C for 30 min. The obtained film was named as M-Fe-3.

Acknowledgements.

L.M. Guo would like to thank JSPS (Japan Society for the Promotion of Science) for a fellowship. This work was supported by the International Institute for Carbon-Neutral Energy Research (WPI-I²CNER), which was established by the World Premier International Research Center Initiative (WPI), MEXT, Japan.

Notes and references

[a]*International Institute for Carbon-Neutral Energy Research (WPI-I²CNER),* [b]*Department of Applied Chemistry and* [c]*International Research Center for Hydrogen Energy, Kyushu University, 744 Motooka, Nishi-ku, Fukuoka 819-0395, Japan.*
[d]*Department of Chemistry, Graduate School of Science, Tohoku University, Aoba-ku, Sendai 980-8578, Japan.*
[*]*E-mail: lmguo1982@gmail.com, teramae@m.tohoku.ac.jp, ishihara@cstf.kyushu-u.ac.jp.*

†Electronic Supplementary Information (ESI) available: Experimental detail, NMR spectra, XRD patterns, SEM images, TEM images, and photochemical performance. See DOI: 10.1039/b000000x/

1. R. Y. Zhang, A. A. Elzatahry, S. S. Al-Deyab, D. Y. Zhao, *Nano Today*, 2012, **7**, 344.
2. F. M. Cui, Z. L. Hua, C. Y. Wei, J. Q. Li, Z. Gao, J. L. Shi, *J. Mater. Chem.*, 2009, **19**, 7632.
3. I. E. Rauda, R. Buonsanti, L.C. Saldarriaga-Lopez, K. Benjauthrit, L. T. Schelhas, M. Stefik, V. Augustyn, J. Ko, B. Dunn, U. Wiesner, D. J. Milliron, S. H. Tolbert, *ACS Nano*, 2012, **6**, 6386.
4. T. Brezesinski, J. Wang, S. H. Tolbert, B. Dunn, *Nat. Mater.*, 2010, **9**, 146.
5. K. Bresesinski, J. Wang, J. Haetge, C. Reitz, S. O. Steinmueller, S. H. Tolbert, B. M. Smarsly, B. Dunn, T. Brezesinski, *J. Am. Chem. Soc.*, 2010, **132**, 6982.
6. T. E. Quickel, V. H. Le, T. Brezesinski, S. H. Tolbert, *Nano Lett.*, 2010, **10**, 2982.
7. T. Bresesinski, J. Wang, R. Senter, K. Brezesinski, B. Dunn, S. H. Tolbert, *ACS Nano*, 2010, **4**, 967.
8. C. Reitz, C. Suchomski, C. Weidmann, T. Brezesinski, *Nano Res.*, 2011, **4**, 414.
9. Y. D. Wang, T. Brezesinski, M. Antonietti, B. Smarsly, *ACS Nano*, 2012, **3**, 1373.
10. J. Haetge, I. Djerdj, T. Brezesinski, *Chem. Commun.*, 2012, **48**, 6726.
11. A. Thomas, H. Schlaad, B. Smarsly, M. Antonietti, *Langmuir*, 2003, **19**, 4455.
12. J. Z. Du, S. P. Armes, *J. Am. Chem. Soc.*, 2005, **127**, 12800.

13. S. J. Hou, E. L. Chaikof, D. Taton, Y. Gnanou, *Macromolecules*, 2003, **36**, 3874.
14. X. P. Dong, H. R. Chen, W. R. Zhao, X. Li, J. L. Shi, *Chem. Mater.*, 2007, **19**, 3484.
15. J. W. Lee, M. C. Orilall, S. C. Warren, M. Kamperman, F. J. Disalvo, U. Wiesner, *Nat. Mater.*, 2008, **7**, 222.
16. L. M. Guo, H. Hagiwara, S. Ida, T. Daio, T. Ishihara, *ACS Appl. Mater. Interfaces*, 2013, **5**, 11080.
17. K. Brezesinski, J. Haetge, J. Wang, S. Mascotto, C. Reitz, A. Rein, S. H. Tolbert, J. Perlich, B. Dunn, T. Bresesinski, *Small*, 2011, **7**, 407.
18. I. Cesar, A. Kay, J. A. G. Martinez, M. Grätzel, *J. Am. Chem. Soc.*, 2006, **128**, 4582.
19. J. Y. Kim, G. Magesh，D. H. Youn, J. W, Jang, J. Kubota, K. Domen, J. S. Lee, Sci. Rep., 2013, 3, 2681.
20. S. C. Warren, K. Voïtchovsky, H. Dotan, C. M. Leroy, M. Cornuz, F. Stellacci, C. Hébert, A. Rothschild, M. Grätzel, *Nat. Mater.*, 2013, **12**, 842.

